

The Effect of Remnant Vortices in He II on Multiple Modes of a Micro-electromechanical Resonator

C. S. Barquist¹ · W. G. Jiang¹ · P. Zheng¹ · Y. Lee¹ · H. B. Chan²

Received: 10 July 2018 / Accepted: 2 December 2018 © Springer Science+Business Media, LLC, part of Springer Nature 2019

Abstract

A micro-electromechanical plate resonator suspended 2 μ m above a substrate was immersed in 4 He at 14 mK at saturated vapor pressure. At these temperatures, four vibrational modes of the device are observed. The corresponding motion of these modes is identified by comparing the observed modes with computer simulations. Owing to its large surface area and small mass, the resonator is sensitive to remnant vortices. The behavior of the modes is studied in the presence of remnant vortices and also in the presence of fully developed turbulence generated by a quartz tuning fork.

Keywords Vortex · Quantum turbulence · Superfluid · ⁴He · He II · MEMS

1 Introduction

Turbulence in superfluid ⁴He (He II) has been an active topic of theoretical, computational, and experimental investigation for several decades [1–3]. At low temperatures when the normal fluid density becomes vanishingly small, turbulence takes the form of a tangle of singly quantized vortex filaments. Mechanical oscillators immersed in the fluid, such as quartz tuning forks [4,5], vibrating wires [6,7], microspheres [8], and oscillating grids [9], have been successfully used to study the behavior of quantized vortices and quantum turbulence.

This work is supported by the National Science Foundation through DMR-1708818.

✓ Y. Lee yoonslee@phys.ufl.eduC. S. Barquist cbarquist@ufl.edu

Published online: 01 February 2019

Department of Physics, The Hong Kong University of Science and Technology, Clear Water Bay, Kowloon, Hong Kong



Department of Physics, University of Florida, Gainesville, FL 32611, USA

In order to better understand how quantum turbulence is generated, it is important to understand the interaction between remnant (trapped) vortices and the device under study. In this paper, we present a comparison of several modes of a microelectromechanical systems (MEMS) device in vacuum at 1 K and in He II at 14 mK. The effect of trapped vortices is manifested as increased damping on the device. When a mode is in the nonlinear Duffing regime, fluctuations in damping arising from trapped vortices can be observed as phase noise of the oscillation relative to the driving force.

2 Experimental Details

The MEMS device used in this study consists of a large $2 \times 125 \times 125 \,\mu\text{m}^3$ center plate suspended $2\,\mu\text{m}$ above a substrate by four springs. A similar device was used extensively to investigate the surface bound states in $^3\text{He-B}$ down to $0.2\,\text{mK}$ [10–12]. The device is driven and detected using comb electrodes attached to the center plate. The detection and actuation scheme used in this study is described in [13] with more in-depth analysis and characterization of similar schemes presented in [14–16]. A rendering of the device without the comb teeth is shown in Fig. 1a.

The geometry of the MEMS device allows multiple resonance modes. The four lowest frequency modes are the Y-pivot (YP), trampoline (TR), X-pivot (XP), and shear modes (SH). The SH mode corresponds to the oscillation parallel to the substrate in the *x*-direction as shown in Fig. 1a, while the TR mode is in the *z*-direction. The XP and YP modes correspond to a rotation about the *x*- and *y*-axis, respectively. An illustration of the corresponding motion of all modes can be seen in [16]. The modes are identified by numerical simulations using COMSOL Multiphysics. The relative phase of the modes also provides further evidence of their correct identification.

Inside of the experimental cell are the MEMS device and a Cernox CR-002RX quartz tuning fork (TF). The TF is located 1 cm above the MEMS device and is mainly used to generate turbulence. This setup allowed the MEMS to be studied in the presence of turbulence generated by the TF and in the presence of remnant vortices pinned to the device after being exposed to the turbulence generated by the TF. Turbulence was generated by driving the TF with increasingly large amplitude until the damping of the TF became nonlinear. This was done by fixing the driving frequency on resonance and ramping the driving excitation while monitoring the velocity of the TF. In the laminar regime, the velocity of the TF is proportional to the driving force. Departure from this linearity and a sudden decrease in the velocity indicate the onset of turbulence [4,5].

In order to find and identify the modes, the excitation frequency was swept from 2 to 24 kHz. This wide range frequency sweep was done in vacuum at 1 K and in He II at 1.8 K and 14 mK. After identifying the modes, detailed sweeps in a narrow range around the peak were made to study each mode. Three modes were observed in vacuum. These modes are identified as the YP, TR, and SH modes with increasing frequency. However, the XP mode, which is predicted by simulation to have a resonance frequency less than the SH mode, was not observed. Due to imperfections in the fabrication process it is possible that the actual resonance frequency is above the range searched.

In He II at 14 mK, all four modes were observed. Due to mass loading, the resonance of each mode is shifted down to a lower frequency. The appearance of the XP mode in



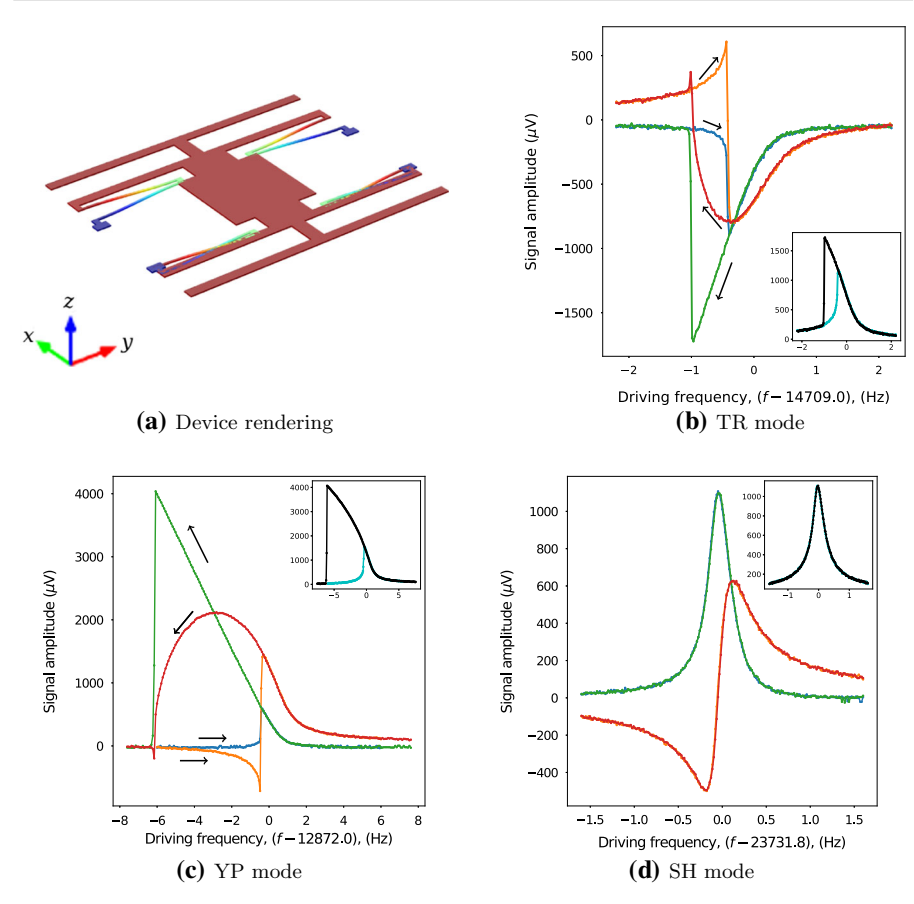


Fig. 1 a A rendering of the MEMS device depicting the SH mode displacement. \mathbf{b} - \mathbf{d} Up and down frequency sweeps of a particular mode in vacuum. In each plot, the x- and y-channels of the signal are displayed along with the amplitude in the inset. The arrows indicate the direction of each frequency sweep (Color figure online)

the frequency range searched is likely due to the enhanced effective mass. In contrast, only the SH was visible when a similar device was measured down to 0.2 mK in ³He-B [10]. This is because the damping in ³He-B is significantly enhanced due to the Andreev reflection process [17]. In He II at 1.8 K only the Y-Pivot and SH modes are observable.

3 Results

3.1 MEMS in Vacuum

Frequency sweeps of each mode found in vacuum are shown in Fig. 1. In the figure, an up-sweep (low to high frequency) and a down-sweep (high to low frequency) are



shown for each mode. Plotted are the in-phase (x-channel) and the out-of-phase (y-channel) components of the output signal from the device, which is proportional to its displacement. The inset shows the amplitude of the signal as a function of frequency. The signals for the TR and YP modes were obtained with a $200\,\mathrm{mV_{pp}}$ excitation, and the SH mode was measured with a $300\,\mathrm{mV_{pp}}$ excitation. In these conditions, both the TR and YP modes are in the nonlinear Duffing regime [18]. However, at this excitation the SH mode still remains linear. A driving force roughly four times greater than the one used here was required before the SH mode entered into the nonlinear regime.

Hysteresis between the up- and down-sweeps is characteristic of the device being in the Duffing regime. When the driving excitation is large enough, the Duffing oscillator exhibits a large jump in amplitude at a specific frequency that depends on the direction of the sweep. The jumps are transitions between bi-stable states of the oscillation [18]. All modes measured display a larger maximum amplitude for a down-sweep when driven in the nonlinear regime. This is indicative of a softening nonlinearity: for larger amplitudes of motion the resonance frequency shifts to lower frequencies. The nonlinear nature of these modes arises from the nonlinearity of the electrostatic force between electrodes for large displacements from equilibrium [19,20]. The nonlinearity is more pronounced for the TR and YP modes because they involve the out-of-plane motion. In vacuum at 1 K, these modes can be driven linearly with an order of magnitude smaller excitation.

3.2 MEMS in He II

Frequency sweeps of the four modes in He II were performed at 14 mK (see Fig.2). All modes were measured with the same excitation of $200\,\text{mV}_{pp}$ and were taken after transferring helium to the dewar. The XP mode is unique because no signal was observed during the up-sweep. This large asymmetry between the up- and downsweeps indicates that the nonlinearity of this mode is more pronounced than the others. In the presence of turbulence generated by the TF, this mode was not observable at all. Even after stopping the generation of turbulence, this mode was completely damped out by the remaining vortices pinned to the device.

In He II, the shifts in resonance frequency of the YP and TR modes are larger than the resonance shift of the SH mode. Because of the large aspect ratio of the device, the modes that involve out-of-plane motion displace significantly more fluid than the SH mode. It is interesting to observe that the signals from the YP and TR modes exhibit a substantial amount of noise in the two quadrature channels but not in the amplitude. This indicates that the noise is mainly in the phase of the oscillation. The phase noise arises probably due to the random nature of the vortices pinned to the device in the nonlinear Duffing regime. Theoretical analysis shows that in the Duffing regime a small change in the damping leads to a change in the phase, while maintaining the same amplitude [18]. Therefore, the phase noise observed could be due to fluctuations in damping caused by fluctuating vortex structure around the device.

After exposing the device to TF turbulence, the phase noise becomes more pronounced. It is believed that the increase in noise is due to an increase in the number of vortices pinned to the device. In a process called *annealing*, the device is swept with



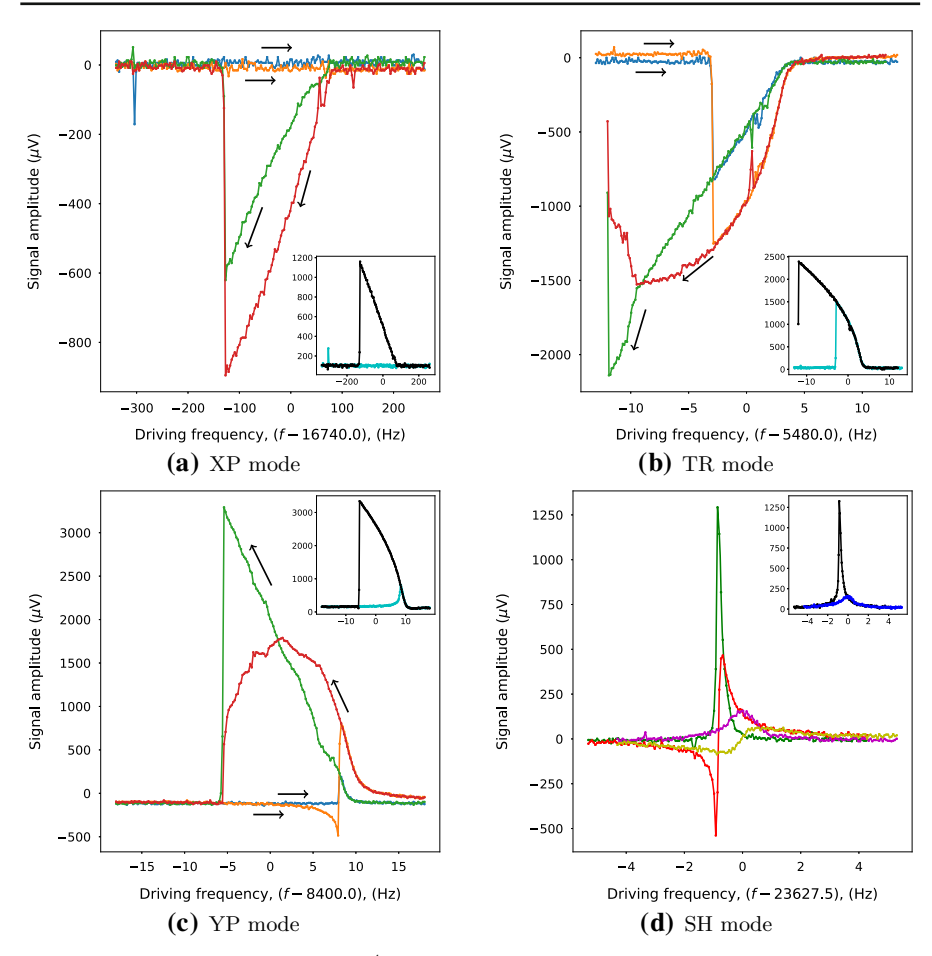


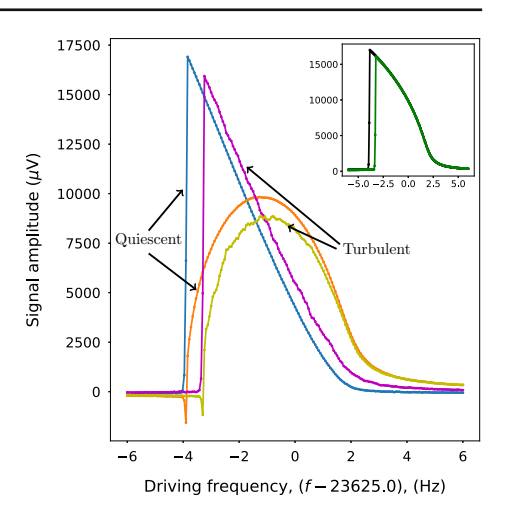
Fig. 2 Frequency sweeps of the modes in ⁴He at 14 mK. **a–c** Up and down frequency sweeps of a particular mode. **d** Two down-sweeps of the shear mode made with the same excitation. In each plot, the *x*- and *y*-channels of the signal are displayed along with the amplitude in the inset. The arrows indicate the direction of each frequency sweep (Color figure online)

large amplitude repeatedly. After annealing the phase noise is dramatically reduced and the resonance becomes sharper. The annealing process is likely removing many of the pinned vortices from the device. When the density of pinned vortices is low, as indicated by a small amplitude of phase noise, it can take up to a day of annealing to further reduce the number of pinned vortices. A typical annealing sweep with the SH has a maximum displacement of about $1.8\,\mu\mathrm{m}$ (or $0.27\,\mathrm{m/s}$).

Figure 2d shows two down-sweeps of the SH mode both made with a $200\,\text{mV}_{pp}$ excitation. The smaller peak is from a measurement made immediately after driving turbulence with the TF, and the larger peak is from a sweep after the annealing process. The increase in pinned vortices after being exposed to turbulence increases the damping on the device and drastically reduces the height of the peak.



Fig. 3 The x- and y-channels of two down-sweeps along with the amplitude in the inset. The *Turbulent* sweep was made in the presence turbulence, and the *Quiescent* sweep was made in its absence (Color figure online)



3.3 Shear Mode Response to TF Trubulence

Figure 3 shows two down-sweeps of the SH mode. Both sweeps were made with $800\,\mathrm{mV_{pp}}$ excitation. One sweep was made in the presence of turbulence and the other in its absence.

There are several features that distinguish the turbulent sweep from the quiescent sweep. The turbulent sweep transitions between bi-stable states of the Duffing oscillator at a higher frequency and lower amplitude, and also has its phase shifted relative to the other sweep. Some small-phase noise can also be seen in the quadrature channels for the turbulent sweep. The maximum amplitude of a Duffing oscillator occurs when the driving force is equal to the damping force. Extra damping on the device from the presence of turbulence causes the bi-stable transition to occur at a lower amplitude for the turbulent sweep. The overall shift in-phase and the increase in frequency of the bi-stable transition are consequences of the transition happening at a lower amplitude. The phase noise during the turbulent sweep is then a result of fluctuations around the average increase in damping. Through its sensitivity to the turbulent damping, the MEMS is sensitive to the average vortex density near the device and fluctuations around this average. A more detailed analysis of the phase noise will be published elsewhere.

4 Conclusion

A micro-electomechanical oscillator was studied in vacuum at 1 K and in He II down to 14 mK. Due to its geometry, the device supports several different resonance modes that undergo unique motions. At 14 mK in He II, all modes have their line shape distorted in the presence of vortices pinned to the device. When driven in the Duffing regime, the MEMS is sensitive to the average vortex density through a shift in the bi-stable transition and to fluctuations in the average vortex density through the phase noise.



References

- 1. C.F. Barenghi, L. Skrbek, K.R. Sreenivasan, PNAS 111, 4647 (2014)
- 2. W. Guo, M.L. Mantia, D.P. Lathrop, S.W. Van Sciver, PNAS 111, 4653 (2014)
- 3. W.F. Vinen, J.J. Niemela, J. Low Temp. Phys. **128**, 167 (2002)
- 4. M. Blažková, M. Človenčko, E. Gažo, L. Skrbek, P. Skyba, J. Low Temp. Phys. 148, 305 (2007)
- D.I. Bradley, M.J. Fear, S.N. Fisher, A.M. Guénault, R.P. Haley, C.R. Lawson, P.V.E. McClintock, G.R. Pickett, R. Schanen, V. Tsepelin, L.A. Wheatland, J. Low Temp. Phys. 156, 116 (2009)
- D.I. Bradley, D.O. Clubb, S.N. Fisher, A.M. Guénault, R.P. Haley, C.J. Matthews, G.R. Pickett, K.L. Zaki, J. Low Temp. Phys. 138, 493 (2005)
- H. Yano, A. Handa, H. Nakagawa, K. Obara, O. Ishikawa, T. Hata, M. Nakagawa, J. Low Temp. Phys. 138, 561 (2005)
- 8. J. Jäger, B. Schuderer, W. Schoepe, Phys. Rev. Lett. **4**, 566 (1995)
- 9. S.I. Davis, P.C. Hendry, P.V.E. McClintock, Physica B 280, 43 (2000)
- 10. P. Zheng, W.G. Jiang, C.S. Barquist, Y. Lee, H.B. Chan, Phys. Rev. Lett. 117, 195301 (2016)
- 11. P. Zheng, W.G. Jiang, C.S. Barquist, Y. Lee, H.B. Chan, Phys. Rev. Lett. 118, 0654301 (2017)
- 12. P. Zheng, W.G. Jiang, C.S. Barquist, Y. Lee, H.B. Chan, J. Low Temp. Phys. 187, 309 (2017)
- C.S. Barquist, P. Zheng, W.G. Jiang, Y. Lee, Y.K. Yoon, T. Schumann, J. Nogan, M. Lilly, J. Low Temp. Phys. 183, 307 (2016)
- 14. P. Zheng, W.G. Jiang, C.S. Barquist, Y. Lee, H.B. Chan, J. Low Temp. Phys. 183, 313 (2016)
- C.S. Barquist, J. Bauer, T. Edmonds, P. Zheng, W.G. Jiang, M. González, Y. Lee, H.B. Chan, J. Phys. Conf. Ser. 568, 032003 (2014)
- 16. M. González, P. Zheng, E. Garcell, Y. Lee, H.B. Chan, Rev. Sci. Instrum. 84, 025003 (2013)
- D.I. Bradley, P. Crookston, S.N. Fisher, A. Ganshin, A.M. Guénault, R.P. Haley, M.J. Jackson, G.R. Pickett, R. Schanen, V. Tseplin, J. Low Temp. Phys. 157, 476 (2009)
- 18. A.H. Nayfeh, D.T. Mook, Nonlinear Oscillators (Wiley-VCH, Weinheim, 2004), pp. 162–165
- E. Collin, M. Defoot, K. Lulla, T. Moutonet, J.-S. Heron, O. Bourgeois, YuM Bunkov, H. Godfrin, Rev. Sci. Instrum. 83, 045005 (2012)
- A.M. Elshurafa, K. Khirallah, H.H. Tawfik, A. Emira, A.K.S.A. Aziz, S.M. Sedky, J. Microelectromech. Syst. 20, 943 (2011)

Publisher's Note Springer Nature remains neutral with regard to jurisdictional claims in published maps and institutional affiliations.

